

Solvation Dynamics in Monohydroxy Alcohols: Agreement between Theory and Different Experiments

Ranjit Biswas, Nilashis Nandi, and Biman Bagchi^{*,†}

Solid State and Structural Chemistry Unit, Indian Institute of Science, Bangalore 560 012, India

Received: August 30, 1996; In Final Form: January 22, 1997[⊗]

Recently three different experimental studies on ultrafast solvation dynamics in monohydroxy straight-chain alcohols (C₁–C₄) have been carried out, with an aim to quantify the time constant (and the amplitude) of the ultrafast component. The results reported are, however, rather different from different experiments. In order to understand the reason for these differences, we have carried out a detailed theoretical study to investigate the time dependent progress of solvation of both an ionic and a dipolar solute probe in these alcohols. For methanol, the agreement between the theoretical predictions and the experimental results [Bingemann and Ernsting *J. Chem. Phys.* **1995**, *102*, 2691 and Horng et al. *J. Phys. Chem.* **1995**, *99*, 17311] is excellent. For ethanol, propanol, and butanol, we find no ultrafast component of the time constant of 70 fs or so. For these three liquids, the theoretical results are in almost complete agreement with the experimental results of Horng et al. For ethanol and propanol, the theoretical prediction for ionic solvation is not significantly different from that of dipolar solvation. Thus, the theory suggests that the experiments of Bingemann and Ernsting and those of Horng et al. studied essentially the *polar* solvation dynamics. The theoretical studies also suggest that the experimental investigations of Joo et al. which report a much faster and larger ultrafast component in the same series of solvents (*J. Chem. Phys.* **1996**, *104*, 6089) might have been more sensitive to the nonpolar part of solvation dynamics than the polar part. In addition, a discussion on the validity of the present theoretical approach is presented. In this theory the ultrafast component arises from almost frictionless inertial motion of the individual solvent molecules in the force field of its neighbors.

I. Introduction

The time dependent solvation of a polar solute in a dipolar solvent has been studied with great interest in the last decade.^{1–17} Since the dynamics of the solvation of a particular species (ion or dipole) can profoundly affect the kinetics of many electron transfer reactions^{6,18,19} occurring in these solvents, a quantitative understanding of the solvent response to an instantaneously created charge distribution in a polar solute is necessary and important to understand the dynamic solvent effects on these reactions. A large number of experimental,^{10,11,20} theoretical,^{21–25} and computer simulation^{26,27} studies have suggested that in many common solvents like water^{23–25} and acetonitrile^{20–22,26,27} the time dependent solvent response to an instantaneously created charge distribution is biphasic with an ultrafast component which carries 60–70% of the total solvation energy with a time constant ranging between 50 and 100 fs. The other component of the biphasic response is rather slow with a time constant in the picosecond range. This ultrafast component in these solvents has been shown to be rather generic in nature which originates from the fast modes of the solvent such as librational and intermolecular vibrational modes.

The scenario appears to be rather different and controversial (at this stage) for the homologous series of the straight chain monohydroxy alcohols. An earlier experimental study²⁸ on solvation dynamics in methanol has shown that it exhibits much slower dynamics where the solvent response to an instantaneously created charge distribution could be given by a biexponential response function with two different time constants in the picosecond regime. However, subsequent theoretical investigations²⁹ and computer simulation studies³⁰ in metha-

TABLE 1: Comparison among the Experimental Time Constants and Amplitudes Reported by the Three Different Experiments

	Joo et al.	Horng et al.	Bingemann et al. ^b
		Methanol	
τ_1 (ps)	0.065	0.03 ^a	0.07
A_1 (%)	52.6	10.1	30.0
		Butanol	
τ_1 (ps)	0.0585	0.243	
A_1 (%)	38.2	15.9	

^a This time constant has been taken arbitrarily since the response was too fast to be detected by the experiment performed by Horng et al. using subpicosecond time resolution. ^b Experimental data for other alcohols have not been reported so far by this group.

nol have indicated the presence of an ultrafast component. This has been confirmed by a series of different experiments^{31–33} performed very recently which shows that in methanol there is indeed an ultrafast component with a time constant of about 70 fs which carries nearly 50% of the total solvation. Although the experimental and computer simulation studies are in agreement with the existing theoretical results for water and acetonitrile, the situation has not been the same for methanol.

Recently solvation dynamics in ethanol, propanol, and butanol have also been investigated experimentally by using nonlinear spectroscopic techniques by different groups.^{31–33} The results obtained are rather different for different experiments. We tabulate the time constants associated with the ultrafast component of the total solvent response function for the four alcohols in Table 1 as obtained by three different experiments to emphasize this point. The obvious disagreement between different experiments for the same alcohols immediately raises the following questions. First, why do these experiments reveal such diverse time scales? Second, which of these experiments correctly probes the dynamical processes that are relevant in

* E-mail address: bbagchi@sscu.iisc.ernet.in.

[†] Also at the Jawaharlal Nehru Center for Advanced Scientific Research, Jakkur, Bangalore.

[⊗] Abstract published in *Advance ACS Abstracts*, March 1, 1997.

determining the polar solvent response to a sudden change in the charge distribution on a dye molecule? Third, is there any relation between the apparently diverse results of these three experiments? Answers to these questions are *crucially* important in determining the dynamic solvent effects on the kinetics of electron transfer reactions and other chemical processes. Note that no theoretical study exists for the solvation dynamics in these three alcohols.

An important feature of some of these experiments is the use of a large dye molecule as a probe. As already mentioned, the techniques applied in these three experiments^{31–33} to follow the time dependent progress of solvation differ from each other. In the experiment of Joo et al.³¹ which uses a dye molecule like IR144 or HITCI as a probe, the time dependent solvent response has been measured by three-pulse-stimulated photon echo peak shift (3PEPS). Here the response function contains a contribution from two potentially different sources. One is the relaxation of the solvation energy, while the second is the equilibrium energy–energy time correlation function. In the experiment of Horng et al.,³² the time dependent progress of the solvation of excited coumarin 153 (C-153) has been followed directly by measuring the usual time dependent Stokes shift of the fluorescence emission spectrum of the probe. On the other hand, Bingemann and Ernsting³³ studied the solvation dynamics of the styryl dye DASPI in methanol. In this experiment, the stimulated emission spectrum has been analyzed by broad-band transient absorption. However, the experimental results for other higher alcohols have not yet been reported by Bingemann and Ernsting.

Clearly, the difference in the results observed may arise at least partly due to the sensitivity of the different experimental techniques to the various aspects of solute–solvent dynamics. A theoretical study of the polar solvation dynamics of an excited solute in these alcohols may answer some of the questions like the presence and amplitude of the ultrafast component in these solvents.

In this paper we present such a theoretical study of *polar* solvation dynamics in methanol, ethanol, propanol, and butanol and compare the theoretical predictions with all the available experimental results.^{31–33} The study reported here has been carried out by using the most recent experimental results of dielectric relaxation in monohydroxy alcohols³⁴ in a simple theoretical approach developed recently. The present study has produced several interesting results. For methanol, the theoretical results are in almost quantitative agreement with the experimental results of Bingemann and Ernsting³³ and are also in satisfactory agreement with results of Horng et al.³² For ethanol, propanol, and butanol, the agreement between the theoretical predictions and the experimental results of Horng et al.³² is also excellent. However, the theoretical results are in total disagreement with the experimental results of Joo et al.³¹ The reason for this is not certain. One possibility is that the results of Joo et al. might be sensitive to the nonpolar part of the solvation whose dynamics is still poorly understood. We shall come back to this point in section V.

The solute probes used in the experimental studies can either be ionic or dipolar in nature. For example, if a well-separated charge transfer complex is formed in the excited state, then the subsequent solvation dynamics can be described as an ionic one. On the other hand, if no charge separation but only charge redistribution takes place on excitation, then the dynamics of solvation of the solute can be regarded as that of a dipole. However, even in the case of coumarin 153, the charge distribution is an extended one with variable charges at different atomic sites. Thus, moments higher than dipole can be

involved.^{14b} This aspect is rather difficult to include in a molecular theory. The calculations for the solvation of the neutral dipole is possible, and the expressions involved are a bit more complicated than those for the ion. In order to understand the results of Horng et al.,³² we have also calculated the solvation energy time correlation function (STCF) for the dipolar solute. The theoretical predictions appear to be in better agreement with the experimental results of Horng et al.³² for ethanol and propanol. For methanol, the long-time decay of the theoretically calculated solvation energy time correlation function for the dipole is also in good agreement with that of Horng et al.³²

The theory used here is rather simple and easy to implement. We have shown earlier that this theory is successful in explaining the experimentally observed solvation dynamics not only in some simple systems like water^{23–25} and acetonitrile^{21,22} but also in amide systems.³⁵ The reason for the success can be attributed to several factors. First, an accurate calculation of the relevant memory function has been carried out by using the full dielectric relaxation data. Second, the *polar* solvation dynamics is found to be dominated by the macroscopic mode of the solvent. This long-wavelength polarization fluctuation has been properly treated by our theory which also systematically includes the effects of short-range local correlations on the generalized rate of polarization relaxation of the solvent. Note that even the moderate success of the continuum model description³⁶ in predicting the qualitative features of the observed solvation dynamics in these polar solvents is entirely due to the dominance of this macroscopic polarization mode. This aspect is also discussed later.

The organization of the rest of the paper is as follows. In the next section we briefly describe the theoretical formulation. Section III contains the details of the calculational procedure. Numerical results on ionic and dipolar solvation dynamics of coumarin-153 alcohols are given in sections IV and V, respectively. In section VI, we try to give a tentative explanation on the origin of the ultrafast component in ethanol and butanol observed by Joo et al.³¹ Section VII ends with a brief discussion.

II. Theoretical Formulation

The solvation time correlation function is defined as usual by the following expression

$$S(t) = \frac{E_{\text{solv}}(t) - E_{\text{solv}}(\infty)}{E_{\text{solv}}(0) - E_{\text{solv}}(\infty)} \quad (1)$$

where $E_{\text{solv}}(t)$ is the time dependent solvation energy of the probe at time t and $E_{\text{solv}}(\infty)$ is the solvation energy at equilibrium. This energy can be obtained by following the time dependent Stokes shift of the emission spectrum after an initial excitation, as in the experiments of Horng et al.³² who used the dye C-153 to obtain the $S(t)$. The time dependent progress of the solvation of a laser-excited dye has also been studied by various highly nonlinear spectroscopic techniques specially suited to study the ultrafast component.³¹ However, these techniques are often to the total energy–energy time correlation function, $M(t)$, defined by the following expression³¹

$$M(t) = \frac{\langle \Delta E(t) \Delta E(0) \rangle}{\langle [\Delta E(0)]^2 \rangle} \quad (2)$$

where $\Delta E(t)$ is the fluctuation in the energy difference between two levels. It is usually stated that $S(t)$ and $M(t)$ are the same *within the linear response* of the liquid. However, different

experiments may be sensitive to different aspects of $S(t)$ and $M(t)$. Thus, while the experiments of Horng et al.³² probe the polar solvation dynamics (that is, $S(t)$) that of Joo et al.³¹ is sensitive to full $M(t)$. For a large dye molecule, this might make a significant difference as discussed below.

In order to study the time dependent progress of solvation in complex systems like alcohols, we need a simple theory that properly includes the dynamic response of the liquid and also the coupling of the probe solute to the solvent. In the following discussions we consider only the polar solvation where the solvation is given by the interaction of the electric field of the polar solute with the polarization field of the dipolar liquid. The present theoretical formulation is based on the well-known density functional theory (DFT) and has been discussed many times earlier,¹ so we give only the bare essentials here. Let us consider a system where the solute ion is translationally mobile and the surrounding dipolar molecules are free to rotate and translate. All these motions can contribute to the process of solvation of the ion. One can then use the DFT to obtain a general free energy function (of density) from statistical mechanics. The free energy function leads to the following expression for the time dependent solvation energy^{37–39}

$$E_{\text{sol}}(r, t) = -k_B T n_{\text{ion}}(\mathbf{r}, t) \int d\mathbf{r}' d\mathbf{\Omega}' c_{\text{id}}(\mathbf{r}, \mathbf{r}', \mathbf{\Omega}', t) \delta\rho(\mathbf{r}', \mathbf{\Omega}', t) \quad (3)$$

where $n_{\text{ion}}(\mathbf{r}, t)$ is the probability that the solute is at position \mathbf{r} at time t and $\delta\rho(\mathbf{r}, \mathbf{\Omega}, t)$ is the fluctuation in the position (\mathbf{r}), orientation ($\mathbf{\Omega}$), and time (t) dependent number density of the dipolar solvent. $c_{\text{id}}(\mathbf{r}, \mathbf{r}', \mathbf{\Omega}')$ is the ion–dipole direct correlation function (DCF).^{40,41} Note that in this expression, the coupling between the ionic solute and the dipolar solvent enters through $c_{\text{id}}(k)$. At a large distance from the solute, this term gives the usual coupling between the electric field of the ion and the dipole moment density. At small distances it includes the molecular aspects and the equilibrium distortion of the solvent due to the polar solute.

Equation 3 leads to an expression of the solvation energy that includes the effects of self-motion of the ion. However, the effect of self-motion is negligible when the solute probe molecule is much heavier and larger than a solvent molecule which is the case considered in all the experiments. Therefore, we shall consider here the solvation of a fixed solute. As a result, the time dependent solvation energy is represented by

$$E_{\text{sol}}(t) = -k_B T \int d\mathbf{r}' d\mathbf{\Omega}' c_{\text{id}}(\mathbf{r}', \mathbf{\Omega}', t) \delta\rho(\mathbf{r}', \mathbf{\Omega}', t) \quad (4)$$

\mathbf{r}' being the position vector from the ion. Next we express eq 4 as an integral over the \mathbf{k} . Spherical harmonic expansions of the c_{id} and $\delta\rho$ and subsequent integration over $\mathbf{\Omega}$ leads to the following expression of the solvation energy

$$E_{\text{sol}}(t) = -k_B T \int d\mathbf{k} c_{\text{id}}^{lm}(k) a_{lm}(\mathbf{k}, t) \quad (5)$$

where c_{id}^{lm} is the (lm) th component of the ion–dipole direct correlation function when expanded in the intermolecular frame and $a_{lm}(\mathbf{k}, t)$ is the (lm) th component of the solvent polarization fluctuation.¹ For solvation of an ion, where only the longitudinal (that, is the $l = 1, m = 0$) component is involved, the equation takes the following form

$$E_{\text{sol}}(t) = -k_B T \int d\mathbf{k} c_{\text{id}}^{10}(k) a_{10}(\mathbf{k}, t) \quad (6)$$

Now, we need the solvation energy–energy time correlation function (EETCF) which will form the basis of our solvation study in these alcohols. It will be denoted by $C_{\text{EE}}(t)$ and is

given as follows

$$C_{\text{EE}}(t) = \frac{(4\pi k_B T)^2}{V} \int_0^\infty dk k^2 |c_{\text{id}}^{10}(k)|^2 \langle a_{10}(-\mathbf{k}) a_{10}(\mathbf{k}, t) \rangle \quad (7)$$

where V is the total volume of the system. $\langle a_{10}(-\mathbf{k}) a_{10}(\mathbf{k}, t) \rangle$ is obtained by using the following expression^{1,21–25}

$$\langle a_{10}(-\mathbf{k}) a_{10}(\mathbf{k}, t) \rangle = \frac{N}{4\pi 3Y} \left[1 - \frac{1}{\epsilon_L(k)} \right] \mathcal{L}^{-1} \left[\frac{1}{z + \Sigma(k, z)} \right] \quad (8)$$

Here, \mathcal{L}^{-1} denotes Laplace inversion with respect to the frequency z , and N represents the total number of molecules present in the system. $3Y$ is the polarity parameter of the pure solvent which can be calculated from the number density (ρ) and dipole moment (μ) of the solvent as follows, $3Y = 4\pi/3 \times (k_B T)^{-1} \mu^2 \rho$. $\Sigma(k, z)$ stands for the wavenumber and frequency dependent generalized rate of solvent polarization relaxation which was shown to be given by^{21–25}

$$\Sigma(k, z) = \frac{2k_B T f_L(k)}{I [z + \Gamma_R(k, z)]} + \frac{k_B T k^2 f_L(k)}{m\sigma^2 [z + \Gamma_T(k, z)]} \quad (9)$$

where I is the average moment of inertia of a solvent molecule of diameter σ and mass m . $\Gamma_R(k, z)$ and $\Gamma_T(k, z)$ are the rotational and the translational dissipative kernels, respectively. Note that eq 9 retains its form when the moment of inertia \mathbf{I} is a tensorial quantity. Then the denominator of the first term is replaced by $\mathbf{I} \cdot [z\mathbf{I} + \mathbf{\Gamma}_R(k, z)]$ where \mathbf{I} is the unit tensor and $\mathbf{\Gamma}_R$ is the dissipative tensor—the rest of the treatment remains unchanged. The longitudinal component of the static structural correlations of the pure solvent is expressed by¹

$$f_L(k) = 1 - \left(\frac{\rho}{4\pi} \right) c(110; k) \quad (10)$$

where $c(110; k)$ denotes the (110)th component of the direct correlation function in the intermolecular frame with \mathbf{k} parallel to the z axis (not to be confused with the Laplace frequency, z). $f_L(k)$ is also related to the longitudinal part of the wave-number dependent dielectric function, $\epsilon_L(k)$, by the following exact relation¹

$$1 - \frac{1}{\epsilon_L(k)} = \frac{3Y}{f_L(k)} \quad (11)$$

The insertion of eq 8 into eq 7 gives the following form of the correlation function

$$C_{\text{EE}}(t) = \frac{(4\pi k_B T)^2 \rho}{4\pi 3Y} \int_0^\infty dk k^2 |c_{\text{id}}^{10}(k)|^2 \left[1 - \frac{1}{\epsilon_L(k)} \right] \mathcal{L}^{-1} \frac{1}{z + \Sigma(k, z)} \quad (12)$$

We now define the normalized solvation energy–energy time correlation function (SETCF) as $M(t) = C_{\text{EE}}(t)/C_{\text{EE}}(t=0)$. At room temperature (which is sufficiently high for the alcohols studied here to make the solvent environment homogeneous as sampled by each solute chromophore),³¹ $M(t) \equiv S(t)$. Consequently, the expression for $M(t)$ can be given as follows

$$M(t) = \frac{\int_0^\infty dk k^2 |c_{\text{id}}^{10}(k)|^2 [1 - 1/\epsilon_L(k)] \mathcal{L}^{-1} [z + \Sigma(k, z)]^{-1}}{\int_0^\infty dk k^2 |c_{\text{id}}^{10}(k)|^2 [1 - 1/\epsilon_L(k)]} \quad (13)$$

Equation 13 is the expression used in the present work to obtain

the normalized solvation energy–energy time correlation function. In this theory, note that $M(t) \equiv S(t)$ as only the *polar* solvation is considered. This $S(t)$ is measured in the time dependent fluorescence Stokes shift (TDFSS) of a probe molecule. Now, the important ingredients to calculate $S(t)$ from eq 13 are the ion–dipole direct correlation function (c_{id}), the static orientational correlation function ($\epsilon_L(k)$), and the memory functions. We shall discuss the calculation procedure of these quantities in the next section.

III. Computational Procedure

A. Calculation of the Static Correlation Functions. The static correlations in these liquids at the intermediate (that is, $k\sigma \approx 2\pi$) to large (that is, $k\sigma > 2\pi$) wavenumbers play an important role in slowing down the rate of solvation at long time. For water, acetonitrile, and methanol, these correlations had been taken from the XRISM calculation of Raineri et al.⁴² However, for these liquids, the solvation was found to be dominated by the long wavelength modes. But for higher alcohols, the solvent structure at small wavelengths (that is, $k\sigma \geq 2\pi$) may also be important. Because of the complexity of these alcohols, a fully microscopic evaluation of the pair correlations appears to be very difficult. However, we found in our earlier studies^{35,39} that even a semiquantitatively accurate $\epsilon_L(k)$ seems capable of producing an accurate $S(t)$, provided proper care is taken to describe this function with the *correct* limiting properties. The two limits which are important are $k = 0$ and $k = 2\pi/\sigma$, where σ is the solvent molecular diameter. For these reasons we have followed the following systematic scheme to find $f_L(k)$ and hence $[1 - 1/\epsilon_L(k)]$. First, we have approximated the alcohol molecules as spheres. At the intermediate wavenumbers, we have taken the orientational correlation functions from the mean spherical approximation (MSA) model.⁴⁰ In the $k \rightarrow 0$ limit, we have used eq 11 to obtain the correct low wavenumber behavior of these static correlations. In the $k \rightarrow \infty$ limits, we have used a Gaussian function which begins at the second peak height of $[1 - 1/\epsilon_L(k)]$ to describe the behavior at large k . This is because, at large k , $f_L(k)$ is a Gaussian function of k .⁴² This Gaussian function has replaced the MSA beyond the second peak of $[1 - 1/\epsilon_L(k)]$ and thereby eliminates the wrong large- k behavior of the MSA. This should be fairly accurate in estimating the electrostatic correlations of these solvents.

We next describe the calculation of the ion–dipole DCF, $c_{id}(k)$. This is taken directly from the solution of Chan et al.⁴¹ of the mean spherical model of an electrolyte solution. We have, of course, used it in the zero-concentration limit. Note that the MSA for the ion–dipole correlation is known to be fairly accurate.⁴³ In the evaluation of $c_{id}(k)$ one requires the knowledge of the solute–solvent size ratio. This is equal to 1.9, 1.67, 1.52, and 1.41 for the solvation of C-153 in methanol, ethanol, propanol, and butanol, respectively. Here the radii of the different solvent and solute molecules have been calculated from their respective van der Waal's molar volumes.⁴⁴ We emphasize here that, because of the properties of $\epsilon_L(k)$ and $c_{id}(k)$, the most important contribution to the correlation function $M(t)$ in eq 13 comes from the $k = 0$ limit where these functions are determined by the macroscopic, well-defined parameters. No adjustable parameters need to be used at any stage of the calculations.

In order to further highlight the role of the long-wavelength polarization modes, we plot in Figure 1 the integrand (in eq 12), $I(k\sigma)$, as a function of $k\sigma$ where $I(k\sigma)$ is defined by

$$I(k\sigma) = (k\sigma)^2 [c_{id}^{10}(k\sigma)]^2 [1 - \epsilon_L(k\sigma)]^{-1} \quad (14)$$

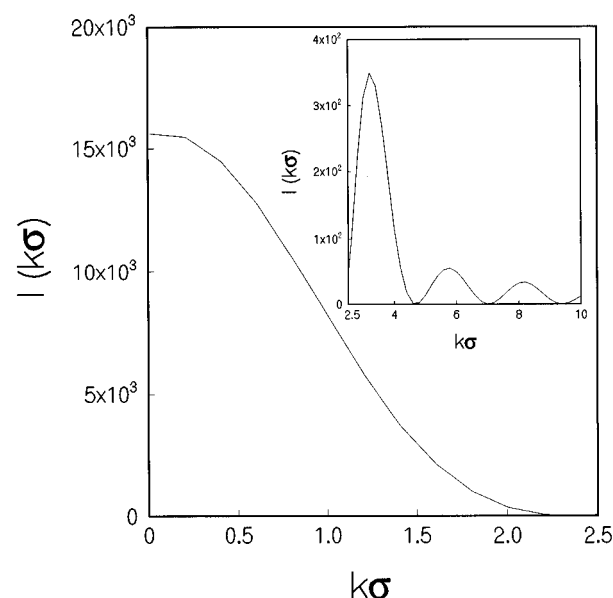


Figure 1. A plot of the wavenumber ($k\sigma$) dependence of the integrand, $I(k\sigma)$ (see eq 14), for ethanol showing the dominance of small wavenumbers in determining the *ionic* solvation energy. In the inset, the wavenumber dependence of the above integrand at $k\sigma > 2.5$ is presented. Note the scale difference along the ordinates of these two graphs. The solvent parameters needed for this calculation are given in Table 2. For discussions, see the text.

TABLE 2: Solvent Parameters Needed for the Theoretical Calculation (Room Temperature Data)

solvent	diameter (Å)	R^a	μ (D)	ρ (g/cm ³)	η (cP)
methanol	4.10	1.9	1.7	0.78	0.5428
ethanol	4.67	1.67	1.69	0.79	1.075
propanol	5.2	1.52	1.7	0.8	2.2275
butanol	5.532	1.41	1.66	0.806	2.271

^a R is the solute–solvent size ratio, calculated for coumarin 153.

where σ is the diameter of a solvent molecule. In Figure 1 the results are for ethanol. The other static parameters such as dipole moment (μ), density (ρ), and static dielectric constant (ϵ_0) needed to characterize the solvent are given in Table 2. This figure clearly shows that the *polar* solvation dynamics derives a major contribution from the long-wavelength (that is, $k\sigma \rightarrow 0$) region. This is because of the long-range nature of the ion–dipole interactions. We shall come back to this point again.

B. Calculation of the Memory Functions. We now discuss the calculational procedure of the memory functions, $\Gamma_R(k,z)$ and $\Gamma_T(k,z)$. These two quantities crucially govern the dynamics of the medium. We have calculated the rotational memory kernel, $\Gamma_R(k,z)$, from the frequency dependent dielectric function, $\epsilon(z)$, after assuming $\Gamma_R(k=0,z) \equiv \Gamma_R(z)$. In our earlier studies^{21–25,35,39,45} this procedure has been found to be successful in explaining the observed solvation dynamics. The relation which connects $\Gamma_R(z)$ with $\epsilon(z)$ is given by the following expression^{21–35}

$$\frac{k_B T}{[z + \Gamma_B(z)]} = \frac{z}{2f_L(0)} \frac{\epsilon_0[\epsilon(z) - \epsilon_\infty]}{\epsilon_\infty[\epsilon_0 - \epsilon(z)]} \quad (15)$$

where ϵ_0 is the static dielectric constant of the medium and ϵ_∞ is the limiting dielectric constant at infrared frequency. $f_L(0)$ is the long-wavelength limit of $f_L(k)$.

The frequency dependent dielectric function, $\epsilon(z)$, for these monohydroxy alcohols is often described by the following rather general expression^{46,47}

$$\epsilon(z) = \epsilon_{\infty} + \sum_{i=1}^m \frac{(\epsilon_i - \epsilon_{i+1})}{[1 + z\tau_i]^{\beta}} \quad (16)$$

where z is the Laplace frequency, ϵ_1 is the static dielectric constant, ϵ_i are intermediate steps in the dielectric constant, $\epsilon_{m+1} = \epsilon_{\infty}$ is its limiting value at high frequency, m is the number of distinct relaxation processes, τ_i are their relaxation time constants, and β is the fitting parameter. For the first three alcohols in this series studied here, an accurate fit is obtained with $\beta = 1$ (that is, Debye processes) and $m = 3$.^{34,48,49} For butanol, $\beta = 0.924$ ⁵⁰ which means a Cole–Davidson model is necessary to describe the relaxation process in this solvent.

For methanol, ethanol, and propanol, we use the most recent dielectric relaxation data measured by Kindt and Schmuttenmaer (KS)³⁴ who used the femtosecond terahertz pulse transmission spectroscopic technique to characterize the multiple Debye behavior of these alcohols. The details of the dielectric relaxation data are summarized in Table 3. The notable aspect of this fs pulse transmission technique is that for the three alcohols studied the measured ϵ_{∞} closely approaches the square of the optical refractive index of the medium, n_D^2 . This suggests that the dielectric relaxation processes observed and characterized by them are complete and reliable. Another interesting aspect of this study is that this technique can precisely detect even a fast process with a time constant of 160 fs (for methanol).

Unfortunately, KS³⁴ did not report $\epsilon(z)$ for butanol. Mashimo et al.⁵⁰ found that for this liquid the relaxation process is a Cole–Davidson one which is responsible for reducing the dielectric constant from 18.32 to 2.72 with a relaxation time constant of 528.4 ps. But the value of the square of the refractive index (n_D^2) for butanol is 1.96. On the other hand, Garg and Smyth⁴⁹ reported a fit by three exponentials with time constants which do not appear to be very reliable.⁵⁰ This indicates that though the first two Debye processes have been successfully fitted to a Cole–Davidson function with the fitting parameter $\beta = 0.924$ by Mashimo et al.,⁵⁰ they missed the last fast process which is responsible for the decrease of the dielectric constant from 2.72 to 1.96. However, it is not difficult to estimate the third time constant by using the results of KS. These authors have already noted that this time constant is rather universal for alcohols. Hence, we attribute this missing region of the dielectric dispersion from 2.72 to 2.22 to a relatively faster Debye relaxation process with a time constant (τ_D) of 2.5 ps. The choice of this τ_D in this range is also supported by the work of Barthel et al.⁴⁸ in propanol where the fastest time constant measured is 2.4 ps. Thus we have supplemented the dielectric relaxation data of Mashimo et al.⁵⁰ with a fast process with a time constant of 2.5 ps.

The translational kernel $\Gamma_T(k, z)$ can be obtained directly from the dynamic structure factor of the liquid using the following expression⁵¹

$$\frac{k_B T}{m\sigma^2 \Gamma_T(k, z)} = \frac{S(k)[S(k) - zS(k, z)]}{k^2 S(k, z)} \quad (17)$$

where the dynamic structure factor is assumed to be given as $S(k, t) = S(k) \exp[-D_T k^2 t / S(k)]$ with D_T as the translational diffusion coefficient of a solvent molecule calculated from the experimentally determined viscosity by using the Stokes–Einstein relation with the slip boundary condition.

IV. Numerical Results: Ionic Solvation

A. Methanol. Let us first discuss the theoretical results on solvation dynamics in methanol. In Figure 2 we show the decay

TABLE 3: Dielectric Relaxation Parameters (Measured at Room Temperature) for the Four Alcohols Studied^a

solvent	processes ^b	ϵ_0	τ_1 (ps)	ϵ_1	τ_2 (ps)	ϵ_2	τ_3 (ps)	ϵ_3	n_D
methanol	3 D	32.63	48	5.35	1.25	3.37	0.16	2.10	1.327
ethanol	3 D	24.35	161	4.15	3.3	2.72	0.22	1.93	1.36
propanol	3 D	20.44	316	3.43	2.9	2.37	0.20	1.97	1.384
butanol ^c	1 D–C	18.38	528.4					2.72	1.40

^a Reference 34 for the first three alcohols. ^b Number of relaxation processes present in the medium; D and D–C correspond to the Debye and Davidson–Cole processes, respectively. ^c $\beta = 0.924$ from ref 50; n_D represents the refractive index of the medium at 598 nm, the sodium D line.

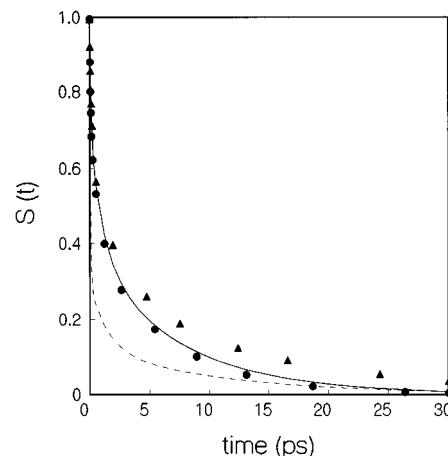


Figure 2. The comparison among the theoretical predictions and three different experimental results for the ionic solvation dynamics of excited C-153 in methanol at room temperature. The solid line represents the calculated normalized solvation energy–energy time correlation function $S(t)$ obtained using eq 13. The experimental results on the same solvent of Horng et al. (ref 32) and Bingemann and Ernsting (ref 33) are represented by filled triangles and filled circles, respectively, while those of Joo et al. (ref 31) are shown by the small dashed line. Note the agreement between the theoretical predictions and the experimental results of Bingemann et al. and Horng et al. A tentative explanation for the reason behind the deviation of the experimental results of Joo et al. from those of Bingemann and Ernsting and Horng et al. is given in section V. The solute–solvent size ratio is 1.9. The dielectric relaxation data and other static parameters needed to calculate $S(t)$ using eq 13 are given in Tables 2 and 3.

of the calculated, normalized solvation time correlation function, $S(t)$, of an ion with time, t . The solute probe is C-153 which was used in the experiment of Horng et al.³² The solute–solvent size ratio is 1.9. For comparison, in the same figure (Figure 2) we also plot the experimental results available from three different experiments, namely those of Joo et al.,³¹ Horng et al.,³² and Bingemann et al.³³ From the figure it is obvious that in methanol, the solvation dynamics is dominated primarily by an ultrafast, Gaussian component. The component with a theoretically calculated ultrafast time constant of about 70 fs accounts for nearly 40–50% of the total solvation. This is in excellent agreement with the experimental results of Bingemann and Ernsting.³³ The decay rate observed by Joo et al.³¹ is considerably faster than the theoretical prediction. The result of Horng et al.,³² on the other hand, is only slightly slower than the theoretical result with an overall good agreement. The exact reason for the deviation from the experimental results of Joo et al.³¹ is not known. This will be discussed later in section V.

Several comments on this almost quantitative agreement between the present theory and the experimental results of Bingemann and Ernsting³³ and of Horng et al.³² are in order. First, this is obtained by using the most recent dielectric relaxation data made available by Kindt and Schmuttenmaer.³⁴

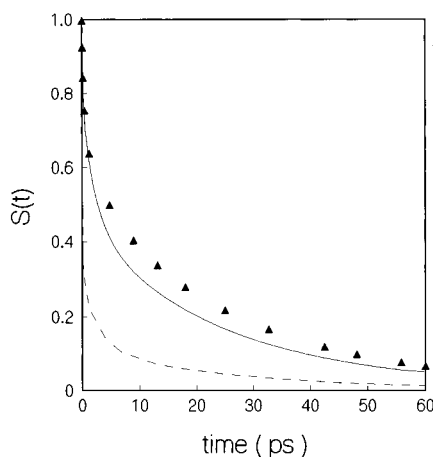


Figure 3. Ionic solvation dynamics of excited C-153 in ethanol at room temperature. The calculated normalized solvation energy-time correlation function, $S(t)$, is shown by the solid line. The experimental results of Horng et al.³² and Joo et al.³¹ are represented by the filled triangles and the small dashed lines, respectively. Here, the solute-solvent size ratio is 1.67. The other necessary parameters needed for the theoretical calculation are given in Tables 2 and 3. For discussions, see the text.

These authors found that in methanol, three consecutive Debye processes bring $\epsilon(z)$ down all the way to 2.1 which is very close to n_D^2 . Thus, no librational mode seems to be significantly coupled to the dielectric relaxation in methanol. If this is indeed correct, then the results obtained here may be the fastest *polar* solvation dynamics present in methanol. Second, it is interesting to contrast this ultrafast solvation dynamics in methanol with that in water and acetonitrile. In water, a very high static dielectric constant ($\epsilon_0 = 78$) coupled with the 193 cm^{-1} intermolecular vibrational band is responsible for the ultrafast solvation, while in acetonitrile, the same is carried out by the extremely fast single-particle rotational motion of the solvent molecules, as probed by the Kerr relaxation.⁵² In methanol, the situation is rather close to acetonitrile in the sense that the ultrafast component here arises from the fast dielectric response of the solvent. Third, no adjustable parameter has been used in the present calculation. Lastly, we have also checked that the calculated $S(t)$ is rather insensitive to the probe size.

B. Ethanol. In Figure 3, we present the theoretical results of solvation dynamics in ethanol. The solute is the same, but now the solute-solvent size ratio is 1.67 due to the larger molecular size of ethanol. In the same figure (Figure 3) we have also plotted the experimental results of Joo et al.³¹ and Horng et al.³² Here the solvation is much slower than that observed in methanol. We also use here, as for methanol, the most recent dielectric relaxation data of Kindt and Schmittenmaer³⁴ (given in Table 3) to obtain the dynamic polar response function of ethanol. However, the solvation is still biphasic which does possess a fast component, but it is not the ultrafast mode in the range of 50–100 fs. The theoretical results are in good agreement with the experimental results of Horng et al.³²

We have the following comments here. First, the excellent agreement observed between the theory and experimental results of Horng et al.³² has been obtained by using the recent dielectric relaxation data.³⁴ These data provide dielectric relaxation down to 1.93 which differs from n_D^2 by only 0.08. Given the very small value of $\epsilon_\infty - n_D^2$, there seems to be little scope of any significant ultrafast component in ethanol, although there can still be a presence of 1–5% of such component if the remaining dispersion ($\epsilon_\infty - n_D^2$) comes from a high-frequency solvent mode. No adjustable parameter has been used in the theoretical calculation.

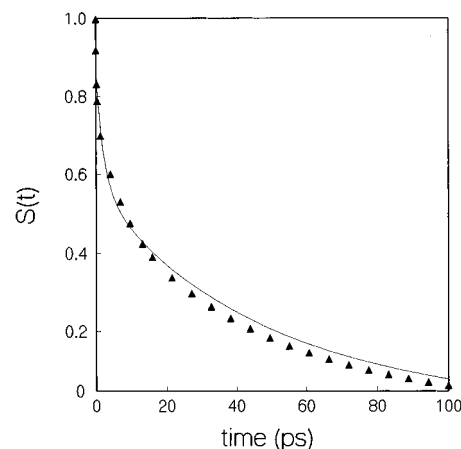


Figure 4. Ionic solvation dynamics of excited C-153 in propanol at room temperature. The theoretical results are shown by the solid line while those of Horng et al.³² are represented by the filled triangles. The solute-solvent size ratio is 1.52. Other static parameters and dielectric relaxation data are given in Tables 2 and 3. For further details, see the text.

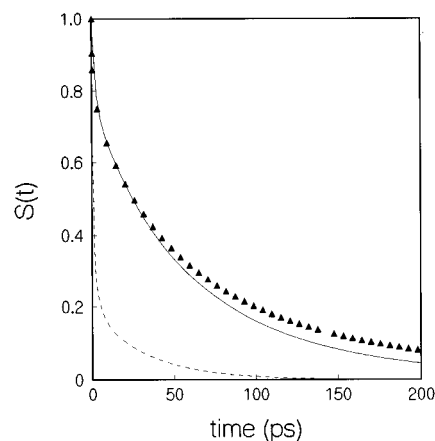


Figure 5. Ionic solvation dynamics of excited C-153 in butanol at room temperature. The solid line represents the theoretical results. The filled triangles and the small dashed lines represent the experimental results of Horng et al.³² and Joo et al.,³¹ respectively. The solute-solvent size ratio is 1.41. The other parameters are given in Tables 2 and 3.

C. Propanol. Next we present the results of the ionic solvation dynamics of coumarin 153 in propanol. The theoretical results are shown in Figure 4. The solute-solvent size ratio is 1.52. Note that here the solvation becomes even slower. This could be attributed to the higher value of the first Debye relaxation time that manifests itself in the slower rotation of a solvent molecule in the hydrogen-bonded pseudocrystalline type network.⁴⁹ We have also plotted the experimental results of Horng et al.³² The agreement is excellent. Here we do not have the results of Joo et al.³¹ Again, no adjustable parameter has been used in the calculation of $S(t)$.

D. Butanol. In Figure 5, we show the results for butanol where the solute-solvent size ratio is now 1.41. For comparison, we have also plotted the experimental results of Joo et al.³¹ and Horng et al.³² The theoretical results are in very good agreement with the experimental results obtained by Horng et al.³² However, the disagreement with that of Joo et al.³¹ is most dramatic in this case.

The following comments on the above results are in order. Unlike the previous cases for methanol, ethanol, and propanol, here the dielectric relaxation data to the degree of desired accuracy are not available. This has led us to approximate the faster solvent response by a time constant of 2.5 ps, taken by

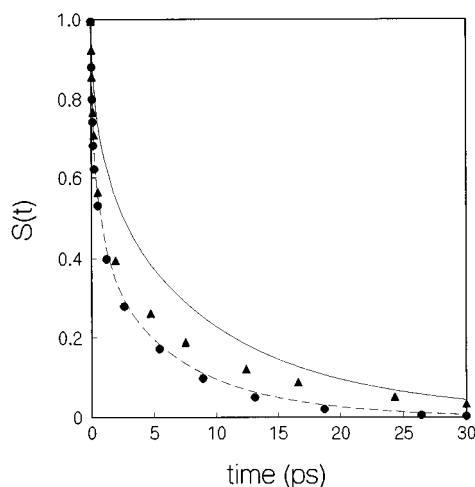


Figure 6. Dipolar solvation dynamics of excited C-153 in methanol at room temperature. The solid line and the dashed line represent the theoretical results on dipolar and ionic solvation dynamics of C-153, respectively. The filled circles and the filled triangles represent the experimental results of Bingemann et al. and Horng et al., respectively.

extrapolating the data of Barthel et al.⁴⁸ This will be discussed in the last section.

V. Numerical Results: Dipolar Solvation

In this section we present the theoretical results of the dipolar solvation dynamics of C-153 in monohydroxy alcohols. The necessary theoretical formulation is given in ref 39. The solvent static parameters and experimental dielectric relaxation data needed for theoretical calculation are given in Tables 2 and 3.

A. Methanol. We first present the results of the dipolar solvation dynamics of C-153 in methanol. In Figure 6 we show the decay of the calculated normalized STCF, $S(t)$, with time, t . For comparison, the experimental results of Bingemann et al.³³ and Horng et al.³² are shown in the same figure (Figure 6). The decay rate of the theoretically predicted $S(t)$ for a dipolar solute (C-153) in methanol, as the comparison indicates, is somewhat slower than that of the experimental results. In fact, the agreement between the theoretical predictions and experimental results becomes better if the solute is assumed to acquire predominantly an ionic character on excitation (see Figure 2). However, an interesting point to note is that the long-time decay of the calculated $S(t)$ for the dipolar solute is now nearly identical to that of Horng et al.³²

B. Ethanol. In Figure 7 we present the theoretical results of the dipolar solvation dynamics of C-153 in ethanol. In the same figure, we have also shown the experimental results of Horng et al.³² The agreement is good. The theoretical results of the ionic solvation dynamics of C-153 in ethanol are again shown in the same figure (Figure 7). Note that there is no significant difference between the theoretically predicted ionic and dipolar solvation dynamics of C-153 in ethanol.

C. Propanol. Next we present the results for propanol. In Figure 8 we show the decay of the theoretically predicted, normalized solvation energy time correlation function, $S(t)$, for propanol with time, t . The experimental results of Horng et al.³² for the same system are also shown in the same figure (Figure 8). The agreement between the theoretical predictions and experimental results is also good here. The theoretical results of the ionic solvation dynamics of C-153 in propanol are presented in the same figure (Figure 8). In propanol also, there is not an appreciable difference between the polar solvent response either to an ionic field or to a dipolar field.

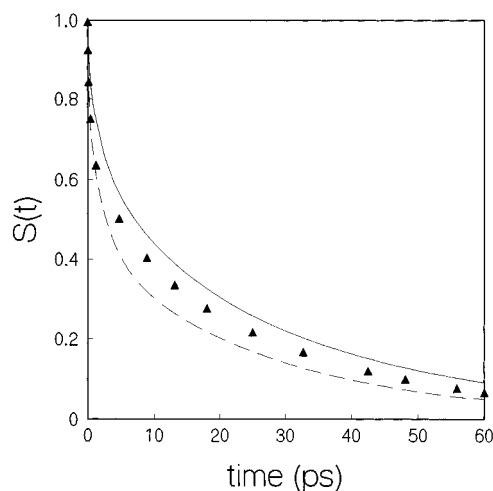


Figure 7. Dipolar solvation dynamics of excited C-153 in ethanol at room temperature. The representations remain the same as Figure 6.

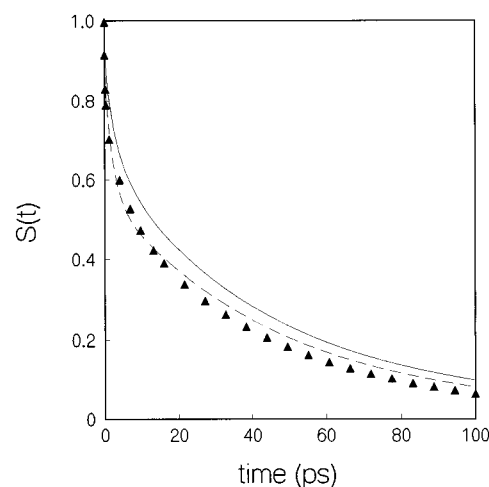


Figure 8. Dipolar solvation dynamics of excited C-153 in propanol at room temperature. The representations remain the same as Figure 6.

It is important to note that there is no significant difference between the ionic and dipolar solvation dynamics of C-153 in ethanol and propanol. This is to be contrasted with the results obtained for water.²⁴ The difference between the two types (ionic and dipolar) of solvation dynamics of a solute probe in a particular solvent strongly depend on the polarity of the medium (quantified by the ϵ_0 and $3Y$ parameters). In weakly polar liquids, the intermolecular correlations and *orientational caging*¹ are not important. However, the translational modes of the solvent can still play a role in the long times.

VI. Can NonPolar Solvation Dynamics Be Responsible for the Ultrafast Component Observed by Joo et al.³¹

As mentioned earlier, the large difference observed among the three experimental results is surprising. Theoretical studies reported here seem to suggest that except for methanol there is no ultrafast component in *polar* solvation dynamics with a time constant of less than 100 fs in normal alcohols. This and the other aspects of the theoretical predictions are in good agreement with the experimental results of Horng et al.³² This, in turn, then implies that the latter work might have explored only the *polar* solvation dynamics in these liquids. This suggestion, in turn, raises two questions. First, what *really* is the origin of the ultrafast component observed in the experiment of Joo et al.³¹ in ethanol and butanol? Second, why does methanol display an ultrafast component whereas the others do not?

It is easy to answer the second question as methanol is much more mobile and possesses a very fast component in dielectric relaxation data which couples to the polarization relaxation through the frequency dependent dielectric function, $\epsilon(z)$. It also has a considerably higher dielectric constant. It is, therefore, not surprising that the *polar* solvation dynamics in methanol would exhibit an ultrafast component.

The answer to the first question on the origin of the ultrafast component observed by Joo et al.³¹ in ethanol and butanol is much more complex. We have the following tentative explanation in terms of nondipolar solvation dynamics.

The dye molecules (HITCI or IR144) used by Joo et al.³¹ are massive with a large surface area, and both contain several aromatic rings. It is known experimentally that these molecules can have an appreciable contribution to the total solvation energy from the nondipolar interactions. One can then divide the total time dependent solvation energy $E_{\text{total}}(t)$ into two parts

$$E_{\text{total}}(t) = E_{\text{NP}}(t) + E_{\text{P}}(t) \quad (18)$$

where the subscripts, P and NP, represent the polar and the nonpolar contribution to the total solvation energy, respectively. Then, the corresponding solvation time correlation functions (unnormalized) are defined as follows

$$S(t) = S_{\text{NP}}(t) + S_{\text{P}}(t) \quad (19)$$

where $S_{\text{NP}}(t) = \langle E_{\text{NP}}(t) E_{\text{NP}}(0) \rangle$ and $S_{\text{P}}(t) = \langle E_{\text{P}}(t) E_{\text{P}}(0) \rangle$. Here, $\langle \dots \rangle$ represents the canonical average, and we have assumed that there is no coupling between the polar and the nonpolar part of the solvation energies. Among the three techniques employed in the nonlinear spectroscopic experiment of Joo et al.,³¹ we shall discuss only the three-pulse-stimulated photon echo peak shift. Here, the time dependence of the peak shift is related to the line-broadening function.^{53,54} The line-broadening function, $g(t)$, is determined both by the magnitude of the Stokes' shift and by the solvation energy time correlation function as follows³¹

$$g(t) = i\lambda_{\text{P}} \int_0^t dt_1 S_{\text{P}}(t_1) + i\lambda_{\text{NP}} \int_0^t dt_1 S_{\text{NP}}(t_1) + \langle |\Delta E_{\text{P}}|^2 \rangle \int_0^t dt_1 \int_0^{t_1} dt_2 S_{\text{P}}(t_2) + \langle |\Delta E_{\text{NP}}|^2 \rangle \int_0^t dt_1 \int_0^{t_1} dt_2 S_{\text{NP}}(t_2) \quad (20)$$

where λ_{P} and λ_{NP} are the reorganization energies which are together responsible for the time dependent shift of the center of the absorbing frequency of the solute probe. ΔE is the fluctuation in the absorption energy due to the fluctuating solvent environment surrounding the chromophore (the probe molecule).

Determination of $g(t)$ requires the values of λ_{X} ($\text{X} = \text{P}, \text{NP}$) and ΔE_{X} for both the polar and nonpolar solvation dynamics. Our reason for presenting eq 20 is to emphasize the point that in 3PEPS and other nonlinear optical techniques, it is not immediately possible to separate the observed response into polar (S_{P}) and nonpolar (S_{NP}) parts. Some recent experimental studies by Berg and co-workers⁵⁵ and Maroncelli and co-workers⁵⁶ have revealed that for nondipolar solvation the frequency shift ranges from 300 to 1000 cm^{-1} . The larger value is obtained when a large probe molecule with aromatic rings is dissolved in polar solvents. The *polar* solvation, on the other hand, gives a shift ranging from 1000 to 2500 cm^{-1} . Since a big dye molecule was used in the experiments of Joo et al.,³¹ a contribution of about 30–60% may easily come from the nonpolar part.^{55,56} This is significant. We next need an estimate of the fastest time scale possible in the nonpolar solvation dynamics. As discussed by several authors,^{55–57} the ultrafast

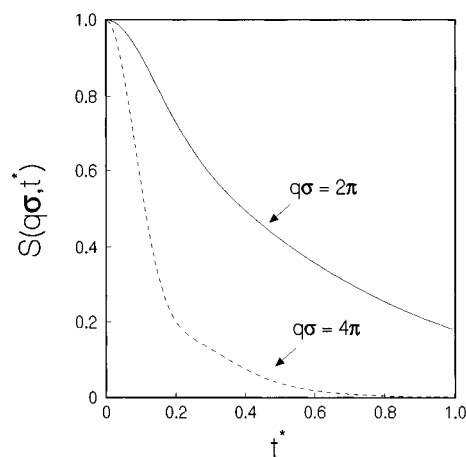


Figure 9. A plot of the normalized solvent dynamic structure factor in the time plane for two wavenumbers. The normalized solvent dynamic structure factor is defined as $S(k, t) = \mathcal{L}^{-1}[S(k, z)/S(k)]$ and calculated from eq 26 for the Lennard–Jones potential. The wavenumber (k) is scaled by the solvent diameter (σ), and the time is scaled by the quantity $[m\sigma^2/k_{\text{B}}T]^{1/2}$. In the calculation, the mass (m) and the diameter (σ) used are those of an ethanol molecule. Note that the decay of $S(k, t)$ at the larger wavenumber is faster than that of the smaller one. In *nonpolar* solvation dynamics, the short time solvent response originates from this type of mechanical and elastic response of the nearest neighbor solvent molecules.

component of the nonpolar solvation dynamics may arise from a mechanical (that is, visco-elastic) response of the liquid. This can indeed be very fast. This may also be due to the fact that many high-frequency intermolecular vibrational modes which are present in a liquid may not couple to the polar solvation dynamics but to the nonpolar solvation dynamics. We next present an analysis of the time constant of the visco-elastic response of the medium.

Theoretical calculation of the nonpolar solvation time correlation function, $S_{\text{NP}}(t)$, has been discussed by several authors.^{55–57} In contrast to the ionic solvation in polar solvents, the nonpolar solvation dynamics is controlled essentially by the dynamic structure factor of the liquid; the orientational relaxation is seen to play a less important role. It has been shown that $S_{\text{NP}}(t)$ is directly proportional to the dynamic solvent structure factor and the final expression is given by the following relation⁵⁷

$$S_{\text{NP}}(t) \propto \int_0^\infty dk k^2 c_{21}^2(k) S(k, t) \quad (21)$$

where c_{21} is the wavenumber (k) dependent direct correlation function between the probe solute (labeled 2) and the solvent molecules (labeled 1). We have calculated the normalized dynamic structure factor, $S(k, t)$ of the solvent at two large wavenumbers—namely, at $k\sigma = 2\pi$ and $k\sigma = 4\pi$, respectively, for a Lennard–Jones liquid at density $\rho\sigma^3 = 0.8$ and temperature $T^* = 2.0$ where $T^* = k_{\text{B}}T/\epsilon$, ϵ being the Lennard–Jones energy parameter. We have used the following dynamic structure factor given by the well-known *Mori continued fraction* which is shown to be expressed as follows^{58–60}

$$S(k, z) = \frac{S(k)}{z + \langle \omega_k^2 \rangle [z + \Delta_k(z + \tau_k^{-1})^{-1}]^{-1}} \quad (22)$$

where ω_k is a wavenumber dependent frequency of the solvent cage, $\Delta_k = \omega_i^2(k) - \langle \omega_k^2 \rangle$, and τ_k is the wavenumber dependent relaxation time defined as $\tau_k = 2(\Delta_k/\pi)^{1/2}$. The details of the definitions are given in the Appendix A. The results are shown for two wavenumbers in Figure 9. It is obvious from the above

figure (Figure 9) that the ultrafast time scale in nonpolar solvation dynamics can indeed originate from the large-wavenumber processes. The $S(k,t)$ at intermediate to large wavenumbers decays with a large rate which in turn can give solvation times around 150–200 fs. This is also the finding of the INM analysis of nonpolar solvation dynamics⁶¹ and also in the experimental studies of nonpolar solvation dynamics in aprotic solvents.⁵⁶ However, this is still longer than the time scale observed by Joo et al.,³¹ and it is unlikely that this mechanism can explain the large amplitude (60–70%) of the ultrafast component. But, this nonpolar mechanism might be present in some other cases where solvation is slow.

Until now we seem to have eliminated both the polar solvation dynamics and the ordinary visco-elastic response of the medium as the probable candidates. We now need to look for a different source to explain the ultrafast component. There are two other possible candidates. One is the suggestion by Ernstring and co-workers that when the time scale of solvation falls below 100 fs, one needs to consider the involvement of vibrational redistribution in the excited state as they can interfere with solvation dynamics in a way which can be indistinguishable from the desired solvent relaxation.^{33b} Unfortunately, we cannot comment on this interesting scenario. The next choice is the one already suggested by Cho et al.⁶² and also by Ladanyi and Stratt.⁶³ For a large dye molecule like HITCI or IR144, a simple calculation shows the 30–40 nearest neighbor solvent molecules may interact directly with the surface of the solute molecule. This may give rise to a contribution of 0.3–0.5 eV in the dispersion energy alone. This can indeed make a large contribution to the equilibrium solvation time correlation function, $\langle \Delta E(t) \Delta E(0) \rangle$. Since alcohols are structured liquids, the molecules next to the probe solute can experience high-frequency motions from the bulk. These motions can easily have frequencies in the 100–1000 cm^{-1} range. Therefore, it is possible to obtain a $M(t)$ which indeed decays very fast, and the experiments of Joo et al.³¹ will be sensitive to this dynamics. This mechanism is quite similar to the nonpolar solvation dynamics discussed above except that it is more sensitive to specific, short-range, solute–solvent interactions.

Clearly, our present understanding of the above is still far from complete. The way the solvation time correlation function was constructed by Horng et al.³² and the time resolution available to them both suggest that they left out such ultrafast nonpolar solvation as discussed above. This certainly explains the agreement with the theory—but we do not yet have a *quantitative* explanation of the ultrafast component observed from 3PEPS measurements in ethanol, propanol, and butanol.

However, if the tentative explanation proposed above in terms of nondipolar, nearest neighbor solute–solvent interactions turns out to be true, then the experiments of Joo et al.³¹ might perhaps by providing us with the much desired information about the dynamics of solute–solvent interactions. This in turn raises the following interesting question: What role would their results play in determining the kinetics of electron transfer reactions occurring in these solvents? If they are not related to dipolar solvation, then one may need to reinvestigate the dynamic solvent effects on the kinetics of these reactions by appropriately generalizing the Marcus model.^{64,65} This ultrafast solvation may very well play the role of nonpolar vibrational modes (the Q-modes) envisaged by Sumi and Marcus in their theory of the electron transfer reaction.^{64b}

VII. Discussion

Let us summarize the main results of this work. We have used a simple molecular theory to study the time dependent

progress of solvation of excited coumarin 153 in the first four members of the homologous series of the straight chain monohydroxy alcohols. The use of this theory has been encouraged by the earlier success of this scheme to study the solvation dynamics not only of water^{23–25} and acetonitrile^{21–22} but also of amides and substituted amides³⁵ at lower temperature. The theoretical predictions are in excellent agreement with the experimental results of Bingemann and Ernstring³³ for methanol and of Horng et al.³² for all the four alcohols. The theory is simple and easy to use. There are certain well-defined approximations but no adjustable parameter.

We find that the solvation dynamics in methanol is primarily governed by the short-time inertial modes of the solvent. The ultrafast, Gaussian component with a time constant of about 70 fs accounts for 40–50 % of the total solvation in this solvent. This is also in good agreement with the experimental results of Bingemann and Ernstring.³³ For the other three alcohols, we do not find any such ultrafast component which is also the observation of Horng et al.³² We have also found that there is no appreciable difference between the dipolar and ionic solvation dynamics of excited coumarin 153 in ethanol and propanol.

The most intriguing part of the present study is the absence of any ultrafast component for polar solvation in ethanol, propanol, and butanol. On the basis of the work reported here, we suggest that the universal ultrafast component observed by Joo et al.³¹ might perhaps be due to nonpolar solvation originating from high-frequency motions of these hydrogen-bonded, nearly polycrystalline liquids.

Let us now comment on the validity of the present hydrodynamic approach to describe the ultrafast *polar* solvation. Our first point concerns the controversy regarding collective versus *single-particle* motion being the crucial step in ultrafast solvation. Here we note that our arguments have been *misunderstood*. We have stated clearly in several places²⁹ that the relevant response function (or, the memory function) of the dipolar liquid that is probed at the ultrafast times is essentially single particle in nature. Since the theory also suggests that at short times translational modes are not important, the relevant motion of a dipolar molecule is then given by the following generalized Langevin equation

$$I \frac{d^2 \rho(\Omega)}{dt^2} = N(\Omega) - \int dt' \Gamma(t-t') \omega(t') + R(t) \quad (23)$$

where the memory function, $\Gamma(t)$, is to be approximated by its short-time limit $N(\Omega)$ is the systematic *torque* acting on the molecule in quation from all other molecules, and $R(t)$ is the random force. ω is the angular velocity. This is the equation of motion used in our calculations with the torque term given by the density functional theory. Note that $\rho(\Omega)$ is the single-particle orientational density. Thus, if we freeze the motion of all other molecules (the *rigid cage* version of Maroncelli⁶⁶), then the equation of motion becomes that of a *free* particle (no friction) *but in the force field of all other molecules of the system*. We have shown elsewhere^{29b} that this leads to a simple and transparent derivation of the relation between the single-particle orientational correlation function and the solvation time correlation function at the short times, recently proposed by Maroncelli and co-workers.^{30b} Thus, there is really no difference between the “single particle” and the collective picture at short times. There is another important issue. As the probe solute is perturbed from its initial state at time $t = 0$, the response of the liquid is largely linear at short times. This response involves the motion of each molecule in the force field of others. In our theory, each molecule behaves as a “free particle” (that is,

experiences no friction) at short times. The small rotation of the solvent molecules leaves the force field on any given molecule essentially time *invariant* during the motion of any molecule. This force can be Fourier decomposed. For dipolar liquids, the long wavelength part of this force (that is, the one involving all the molecules) has the largest force constant. Thus, the long wavelength polarization relaxation is the fastest and gives rise to the ultrafast solvation. Single-particle motion alone (without this collective force field) will *never* give rise to the observed amplitude for the ultrafast polar solvation.

Secondly, we consider the relative importance of the bulk polarization versus the *nearest neighbor* contribution. The bulk polarization mode of our theory is essentially the same mode that appears in the continuum model discussions. It is certainly correct that the long-wavelength longitudinal polarization modes in water, acetonitrile, and methanol decay in the same ultrafast time scale as found in the experiments. This can be proved rigorously by using expressions which involve only macroscopic variables and so does not involve any assumption or use of any microscopic argument. So, the question then comes down to the relative importance of the long-wavelength modes in solvation dynamics. In the present and related theories, the long-wavelength modes together make a large contribution to the total solvation energy because of the long-range nature of the ion–dipole interaction.

It should be pointed out that for *ionic* solvation, computer simulation studies of a small system can run into difficulties. In the language of the present theory, the simulation studies of a small system would mean the truncation of all the modes with wavenumbers between zero and a number which can be rather high. Note that in simulations the situation is further complicated because the probe solute is often placed in the center of the system, thus further curtailing the length of the allowed solvent polarization by half. Thus, there is always this danger that the computer simulation studies of *polar* solvation dynamics, particularly of an ion, may lead to the conclusion that only the nearest neighbor molecules are important and the contribution of the bulk is negligible. The situation is different for dipolar solvation where the system size dependence could be weak.

The above discussion is not meant to suggest that the nearest neighbor molecules do not contribute significantly and that their dynamics is not in the ultrafast time scales. Rather, our aim is to caution the reader about the possible error that may easily arise in the simulations of *polar* liquids, especially in the study of the solvation dynamics of a foreign solute. In the present theory, the relaxation at the lowest wavenumber (around $k\sigma = 1$) accessible in the solvation simulation of 255 molecules (plus the probe solute) is almost of the same time constant as that of $k = 0$. For example, the short-time rate of the wavenumber dependent solvent polarization relaxation, $\Sigma(k\sigma, z)$ (see eq 9) at $k\sigma = 1$ is only $\sim 10\%$ smaller than that at $k\sigma = 0$. Actually this weak wavenumber dependence of relaxation rate is the reason for the dominance by the long wavenumber modes and is also the reason (in the theory) why the ultrafast component dominates in water, acetonitrile, and methanol. In fact, in the simulation studies of ionic solvation dynamics in acetonitrile,⁶⁶ Maroncelli had already noted the dominance by the longest wavelength mode (see Figure 11 of ref 66).

The above discussion has been made more quantitative by plotting the generalized rate of solvent polarization relaxation, $\Sigma(k\sigma, z)$ (of eq 9), against the wavenumber, $k\sigma$. This is shown in Figure 10 for two limits of frequency, z . The results are for ethanol. Note that for both low and high frequencies the wavenumber dependence is rather weak, as noted earlier. The pronounced flatness at low frequency is due to the contribution

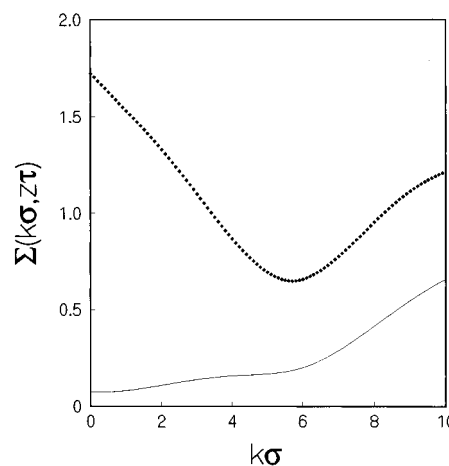


Figure 10. A plot of the calculated wavenumber ($k\sigma$) and frequency (z) dependent generalized rate, $\Sigma(k\sigma, z\tau)$, of the solvent polarization relaxation for two limits of frequency. The results are obtained for ethanol using eq 9. The filled diamonds represent the wavenumber dependence of the generalized rate at a very high frequency, whereas the solid line describes the same at a very low frequency. Note that z is scaled by τ which is equal to 1×10^{-12} s. For discussions, see the text.

of translational modes which becomes relevant as the orientational relaxation becomes slow. This is because in ethanol the single-particle orientation is slow, as evident from the large value for τ_1 (see Table 3). The rate, $\Sigma(k\sigma, z)$, at the intermediate wavenumber is slower than at all other wavenumbers. So, computer simulation studies in a finite system may probe this slower decay. However, this is perhaps not greatly significant as the wavenumber dependence itself is weak.

As already pointed out, the solutes that are routinely used as probes are of complicated shapes. In addition, they undergo complex changes in their charge redistribution upon excitation. The solvation dynamics of such a complex charge distribution can be rather different from that of an ion or a dipole, particularly at short times where the nearest neighbor molecules would react to the extended charge distribution in a way that could be entirely different from what expected from the simple model calculation. The field from a complex charge distribution can entirely be represented by a multipolar expansion, the convergence of which is, however, not clear. In light of this ambiguous situation, the theoretical results obtained here, that at least for alcohols, the solvation dynamics of an ion is not significantly different from that of a dipole, is important and reassuring from a theoretical point of view.

Lastly, the results that are presented are obtained with no adjustable parameter. The near-perfect agreement obtained between theory and experiments for a large number of systems studied so far—water, acetonitrile, amides, and Brownian dipolar lattice—suggest that the present theory is capable of accurately describing *polar* solvation dynamics in dipolar liquids.

The present work suggests the following future problems for experimental study. First, it will be useful to perform both the dielectric relaxation and TDFSS experiments over a wide range of temperature in alcohols. Second, dielectric relaxation using the tera-hertz technique for butanol and higher alcohols are needed. In addition, the effects of ultrafast nonpolar solvation dynamics on electron transfer reactions is an interesting theoretical problem.

Acknowledgment. It is a pleasure to thank Ms. N. Gayathri for many discussions. We thank Prof. W. Jarzeba for several illuminating discussions and for pointing out useful references. We thank Prof. M. Maroncelli, Prof. M. Berg, Prof. R. M. Stratt,

and Prof. B. M. Ladanyi for useful correspondence and helpful suggestions. We are particularly thankful to Prof. M. Maroncelli for motivating us to study the dipolar solvation dynamics (section V). We are grateful to Prof. I. Ohmine, Dr. H. Heitele, and Prof. M. Tachiya for helpful discussions. A part of this work was done when B.B. was visiting the Department of Physical Chemistry, National Institute of Materials and Chemical Research, Tsukuba, Japan, and he thanks the faculty of NIMCR for their kind hospitality. The partial financial supports from the Council of Scientific and Industrial Research, India, and the Indo-French Center for Promotion of Scientific Research, New Delhi, are gratefully acknowledged.

Appendix A

In order to calculate $S(k, t)$, we use the following dynamic structure factor obtained from visco-elastic approximation given by the Mori continued fraction^{58–60}

$$S(k, z) = \frac{S(k)}{z + \langle \omega_k^2 \rangle [z + \Delta_k(z + \tau_k^{-1})^{-1}]^{-1}} \quad (24)$$

where $S(k)$ is the static structure factor obtained using the Weeks–Chandler–Andersen scheme.⁶⁷ The details regarding the calculation of the other static quantities have been discussed elsewhere,⁶⁸ and here we give only the necessary expressions. $\langle \omega_k^2 \rangle = k_B T q^2 / m S(k)$, and $\Delta_k = \omega_1^2(k) - \langle \omega_k^2 \rangle$ where $\omega_1^2(k)$ is the second moment of the longitudinal current correlation function given by^{58–60}

$$\omega_1^2(k) = 3m^{-1}k^2k_B T + \omega_0^2 + \gamma_d^1(k) \quad (25)$$

where the longitudinal component of the vertex function, $\gamma_d^1(k)$, and the Einstein frequency of the solvent, ω_0 , can be calculated from the interacting potential, $v(r)$, and the radial distribution function, $g(r)$, from the following expressions^{58–60}

$$\gamma_d^1(k) = -m^{-1} \rho \int d\mathbf{r} \exp(-i\mathbf{k} \cdot \mathbf{r}) g(r) \frac{\delta^2}{\delta z^2} (v(r)) \quad (26)$$

and

$$\omega_0^2 = 3m^{-1} \rho \int d\mathbf{r} g(r) \nabla^2 v(r) \quad (27)$$

Here, we assume that the interacting potential, $v(r)$, is that given by the Lennard–Jones potential, and then τ_k can be obtained from the relation, $\tau_k = 2(\Delta_k/\pi)^{1/2}$. Thus, once Δ_k and ω_0 is calculated, we put these quantities back in eq 26 and Laplace invert it numerically⁶⁹ to obtain $S(k, t)$.

Note Added in Proof. When this paper was in press, we became aware of an interesting work by Stephens, Saven, and Skinner.⁷⁰ In this work, Stephens et al. have studied the dynamics of nonpolar solvation in the context of electronic line shape, by using both analytical theory and molecular dynamics simulations. The systems studied were simple Lennard–Jones. An important observation of this work is that nonpolar solvation dynamics is initially Gaussian with a time constant in the range of 250–300 fs, depending on the density and the temperature of the liquid. This result is in good agreement with the analysis presented in the section VI of the present article.

References and Notes

- (1) Bagchi, B. *Annu. Rev. Phys. Chem.* **1989**, *40*, 115. Bagchi, B.; Chandra, A. *Adv. Chem. Phys.* **1991**, *80*, 1.

- (2) Maroncelli, M. *J. Mol. Liq.* **1993**, *57*, 1.
- (3) Fleming, G. R.; Wolyne, P. G. *Phys. Today* **1990**, *43*, 36.
- (4) Maroncelli, M.; McInnis, J.; Fleming, G. R. *Science* **1989**, *243*, 1674.
- (5) Barbara, P. F.; Jarzeba, W. *Adv. Photochem.* **1990**, *15*, 1.
- (6) Rossky, P. J.; Simon, J. D. *Nature* **1994**, *370*, 263.
- (7) Gauduel, Y. *J. Mol. Liq.* **1995**, *63*, 1.
- (8) See the articles in *Ultrafast Reaction Dynamics and Solvent Effects*; Gauduel, Y., Rossky, P. J., Eds.; AIP Press: New York, 1994.
- (9) Rosenthal, S. J.; Xie, X.; Du, M.; Fleming, G. R. *J. Chem. Phys.* **1991**, *94*, 4715.
- (10) Jimenez, R.; Fleming, G. R.; Kumar, P. V.; Maroncelli, M. *Nature* **1994**, *369*, 471.
- (11) Raineri, F. O.; Zhou, Y.; Friedman, H. L. *Chem. Phys.* **1991**, *152*, 201.
- (12) Raineri, F. O.; Resat, H.; Perng, B. C.; Hirata, F.; Friedman, H. L. *J. Chem. Phys.* **1994**, *100*, 1477. Raineri, F. O.; Zhou, Y.; Friedman, H. L.; Stell, G. *Chem. Phys.* **1991**, *152*, 201.
- (13) Ladanyi, B.; Skaf, M. S. *Annu. Rev. Phys. Chem.* **1993**, *44*, 335. Fonseca, T.; Ladanyi, B. M. In *Condensed Matter Physics Aspects of Electrochemistry*; Tosi, M. P., Kornyshev, A. A., Eds.; World Scientific: Singapore, 1991.
- (14) (a) Friedrich, V.; Kivelson, D. *J. Chem. Phys.* **1987**, *86*, 6425. (b) Alavi, D. S.; Waldeck, D. H. *J. Chem. Phys.* **1991**, *94*, 6196. Alavi, D. S.; Waldeck, D. H. *Understanding Chemical Reactivity*; Kluwer: Amsterdam, 1994; p 249. Kurnikova, M. G.; Waldeck, D. H.; Coalson, R. D. *J. Chem. Phys.* **1996**, *105*, 628.
- (15) Hynes, J. T. In *Ultrafast Dynamics of Chemical Systems*; Simon, J. D., Ed.; Kluwer: Dordrecht, The Netherlands, 1994; p 345. Smith, B. B.; Kim, H. L.; Borgis, D.; Hynes, J. T. In *Dynamics and Mechanism of Photoinduced Charge Transfer and Related Phenomena*; Mataga, N., Okada, T., Masuhara, H., Eds.; Elsevier: Amsterdam, 1992; p 39.
- (16) Loring, R. F.; Mukamel, S. *J. Chem. Phys.* **1987**, *86*, 6425. Fried, L.; Mukamel, S. *J. Chem. Phys.* **1990**, *93*, 932.
- (17) Wei, D.; Patey, G. N. *J. Chem. Phys.* **1990**, *93*, 1399. Wei, D.; Patey, G. N. *J. Chem. Phys.* **1989**, *91*, 7113. Attard, P.; Wei, D.; Patey, G. N. *Chem. Phys. Lett.* **1990**, *172*, 69. Olender, R.; Nitzan, A. *J. Chem. Phys.* **1995**, *102*, 7180. Chandra, A.; Wei, D.; Patey, G. N. *J. Chem. Phys.* **1993**, *99*, 4926. Chandra, A.; Patey, G. N. *J. Chem. Phys.* **1994**, *100*, 1552. Chandra, A. *Chem. Phys.* **1995**, *195*, 93.
- (18) Heitele, H. *Angew. Chem., Int. Ed. Engl.* **1993**, *32*, 359.
- (19) Weaver, M. J. *Chem. Rev.* **1992**, *92*, 463; Weaver, M. J.; McManis, G. E., III *Acc. Chem. Res.* **1990**, *23*, 294. Roy, S.; Bagchi, B. *J. Chem. Phys.* **1994**, *98*, 9207. Bagchi, B. *Int. Rev. Phys. Chem.* **1987**, *6*, 1.
- (20) Cho, M.; Rosenthal, S. J.; Scherer, N. F.; Ziegler, L. D.; Fleming, G. R. *J. Chem. Phys.* **1992**, *96*, 5033.
- (21) Roy, S.; Komath, S.; Bagchi, B. *J. Chem. Phys.* **1993**, *99*, 3139.
- (22) Komath, S. S.; Bagchi, B. *J. Chem. Phys.* **1993**, *98*, 8987.
- (23) Roy, S.; Bagchi, B. *J. Chem. Phys.* **1993**, *99*, 9938.
- (24) Nandi, N.; Roy, S.; Bagchi, B. *J. Chem. Phys.* **1995**, *102*, 1390.
- (25) Roy, S.; Bagchi, B. *J. Chem. Phys.* **1993**, *98*, 1310.
- (26) Bader, J. S.; Chandler, D. *Chem. Phys. Lett.* **1989**, *157*, 501.
- (27) Maroncelli, M.; Fleming, G. R. *J. Chem. Phys.* **1988**, *89*, 5044.
- (28) Kahlow, M. A.; Jarzeba, W.; Kang, T. G.; Barbara, P. F. *J. Chem. Phys.* **1989**, *90*, 151.
- (29) (a) Roy, S.; Bagchi, B. *J. Chem. Phys.* **1994**, *101*, 4150. (b) Roy, S.; Bagchi, B. *Chem. Phys.* **1994**, *183*, 207.
- (30) (a) Maroncelli, M.; Kumar, P. V.; Papazyan, A.; Horng, M. L.; Rosenthal, S. J.; Fleming, G. R. In *Ultrafast Reaction Dynamics and Solvent Effects*; Gauduel, Y., Rossky, P. J., Eds.; AIP Press: New York, 1994; p 310. (b) Maroncelli, M.; Kumar, P. V.; Papazyan, A. *J. Phys. Chem.* **1993**, *97*, 13. (c) Kumar, P. V.; Maroncelli, M. *J. Chem. Phys.* **1995**, *103*, 3038.
- (31) Joo, T.; Jia, Y.; Yu, J.-Y.; Lang, M. J.; Fleming, G. R. *J. Chem. Phys.* **1996**, *104*, 6089.
- (32) Horng, M. L.; Gardecki, J. A.; Papazyan, A.; Maroncelli, M. *J. Phys. Chem.* **1995**, *99*, 17311.
- (33) (a) Bingemann, D.; Ernsting, N. P. *J. Chem. Phys.* **1995**, *102*, 2691. (b) Ernsting, N. P.; Konig, N. E.; Kemeter, H.; Kovalenko, S.; Ruthmann, J. *Fast Elementary Processes in Chemical and Biological Systems*, AIP Conference Proceedings, Tramer, A., Ed.; AIP Press: New York, 1995; p 441.
- (34) Kindt, J. T.; Schmittenmaer, C. A. *J. Phys. Chem.* **1996**, *100*, 10373.
- (35) Biswas, R.; Bagchi, B. *J. Phys. Chem.* **1996**, *100*, 1238.
- (36) Rips, I.; Klafter, J.; Jortner, J. *J. Chem. Phys.* **1988**, *88*, 3246. Rips, I.; Klafter, J.; Jortner, J. *J. Chem. Phys.* **1989**, *89*, 4288.
- (37) Kirkpatrick, T. R.; Nieuwoudt, J. C. *Phys. Rev. A* **1986**, *33*, 2651.
- (38) Biswas, R.; Roy, S.; Bagchi, B. *Phys. Rev. Lett.* **1995**, *75*, 1098.
- (39) Indrani, A. V.; Ramaswamy, R. *Phys. Rev. Lett.* **1994**, *73*, 360.
- (40) Gray, C. G.; Gubbins, K. E. *Theory of Molecular Fluids*; Clarendon: Oxford, 1984; Vol. I.
- (41) Chan, D. Y. C.; Mitchell, D. J.; Ninham, B. W. *J. Chem. Phys.* **1979**, *70*, 2946. Blum, L. *J. Chem. Phys.* **1974**, *61*, 2129.

- (42) Raineri, F. O.; Resat, H.; Friedman, H. L. *J. Chem. Phys.* **1992**, 97, 3058.
- (43) Wertheim, M. S. *J. Chem. Phys.* **1971**, 55, 4291.
- (44) Edwards, J. T. *J. Chem. Educ.* **1970**, 47, 261.
- (45) Roy, S.; Bagchi, B. *Chem. Phys.* **1994**, 183, 207.
- (46) See for example: *Theory of Electric Polarization*, 78th ed.; Bottcher, C. J. F., Bordewijk, P., Eds.; Elsevier: Amsterdam, 1978; Vol. II.
- (47) Barthel, J.; Buchner, R. *Pure Appl. Chem.* **1991**, 63, 1473.
- (48) Barthel, J.; Bachhuber, K.; Buchner, R.; Gill, J. B.; Hetzenauer, H. *Chem. Phys. Lett.* **1990**, 165, 369.
- (49) Garg, S. K.; Smyth, C. P. *J. Phys. Chem.* **1965**, 69, 1294.
- (50) Mashimo, S.; Kuwabara, S.; Yagihara, S.; Higasi, K. *J. Chem. Phys.* **1989**, 90, 3292.
- (51) Ravichandran, S.; Roy, S.; Bagchi, B. *J. Phys. Chem.* **1995**, 99, 2489.
- (52) Ravichandran, S.; Bagchi, B. *Int. Rev. Phys. Chem.* **1995**, 14, 271.
- (53) McMorrow, D.; Lotshaw, W. T. *J. Phys. Chem.* **1991**, 95, 10395.
- (54) Mukamel, S. *Principles of Non-linear Spectroscopy*; Oxford: New York, 1995.
- (55) Mukamel, S. *Annu. Rev. Phys. Chem.* **1990**, 41, 647.
- (56) Yan, Y. J.; Mukamel, S. *J. Chem. Phys.* **1991**, 94, 179.
- (57) Kubo, R. *Adv. Chem. Phys.* **1969**, 15, 101.
- (58) Ma, J.; Bout, D. V.; Berg, M. *J. Chem. Phys.* **1995**, 103, 9146.
- (59) Berg, M. *Chem. Phys. Lett.* **1994**, 228, 317.
- (60) Ma, J.; Bout, D. V.; Berg, M. Solvation Dynamics Studied by Ultrafast Transient Hole Burning. *J. Mol. Liq.*, in press.
- (61) Fourkas, J. T.; Benigno, A.; Berg, M. *J. Chem. Phys.* **1993**, 99, 8552.
- (62) Fourkas, J. T.; Berg, M. *J. Chem. Phys.* **1993**, 98, 7773.
- (63) (a) Reynolds, L.; Gardecki, J. A.; Frankland, S. J. V.; Horng, M. L.; Maroncelli, M. *J. Phys. Chem.* **1996**, 100, 10337. (b) Saven, J. S.; Skinner, J. L. *J. Chem. Phys.* **1993**, 99, 4391.
- (64) Bagchi, B. *J. Chem. Phys.* **1994**, 100, 6658.
- (65) Boon, J. P.; Yip, S. *Molecular Hydrodynamics*; McGraw-Hill: New York, 1980 and references therein.
- (66) Chandrasekhar, S. *Rev. Mod. Phys.* **1943**, 15, 1.
- (67) Balucani, U.; Zoppi, M. *Dynamics of the Liquid State*; Clarendon Press: Oxford, 1994 and references therein.
- (68) Stratt, R. M.; Cho, M. *J. Chem. Phys.* **1994**, 100, 6700.
- (69) Cho, M.; Fleming, G. R.; Saito, S.; Ohmine, I.; Stratt, R. M. *J. Chem. Phys.* **1994**, 100, 6672.
- (70) Ladanyi, B. M.; Stratt, R. M. *J. Chem. Phys.* **1995**, 99, 2502.
- (71) (a) Marcus, R. A. *J. Chem. Phys.* **1956**, 24, 966. Marcus, R. A. *J. Chem. Phys.* **1956**, 24, 979. (b) Sumi, H.; Marcus, R. A. *J. Chem. Phys.* **1986**, 84, 4272.
- (72) Marcus, R. A. *Annu. Rev. Phys. Chem.* **1964**, 15, 155.
- (73) Maroncelli, M. *J. Chem. Phys.* **1991**, 94, 2084.
- (74) Weeks, J. D.; Chandler, D.; Andersen, H. C. *J. Chem. Phys.* **1971**, 54, 5237.
- (75) Chandler, D.; Weeks, J. D. *Phys. Rev. Lett.* **1970**, 25, 149.
- (76) Bhattacharyya, S.; Bagchi, B. *J. Chem. Phys.* **1996**, 106, 1757.
- (77) Stehfest, H. *Commun. ACM* **1970**, 13, 624.
- (78) Stephens, M. D.; Saven, J. G.; Skinner, J. L. *J. Chem. Phys.*, in press.